Supplementary Information (SI) for Journal of Materials Chemistry A.

SUPPORTING INFORMATION

Laponite nanoclay as a solid-state charge transfer mediator for piezocatalytic hydrogen evolution

Talha Kuru[a,b], Emre Aslan[c], Imren Hatay Patir[a]*

[a] Selcuk University, Department of Biotechnology, 42030, Konya, Türkiye, e-mail: imrenhatay@gmail.com

[b] YEO Technology R&D Center, 34870, İstanbul, Türkiye

[c] Selcuk University, Department of Biochemistry, 42030, Konya, Türkiye, e-mail emreaslan89@gmail.com

Calculation of Mechanical Energy Harvested by the Piezocatalytic Reactor

E_{mech} can be calculated through a sequential integration of physical relationships involving energy transmission within the ultrasonic system. In this setup, water inside the ultrasonic bath (Bandelin RK 255 H) serves as the medium through which mechanical energy is transmitted. The internal dimensions of the water compartment are specified as length **(l)** = 30.0 cm, width **(w)** = 15.0 cm, and depth **(h)** = 3.5 cm, defining the effective transmission volume **(V_0)** as:

$$V_0 = l \times w \times h$$

In these calculations, ρ and c represent the density and the speed of sound of the medium, respectively. The acoustic reflectance **(R)** of the reactor interface against ultrasonic propagation is expressed as:

$$R = \frac{\rho_{borosilicate\ glass} \cdot c_{borosilicate\ glass} - \rho_{water} \cdot c_{water}}{\rho_{borosilicate\ glass} \cdot c_{borosilicate\ glass} + \rho_{water} \cdot c_{water}}$$

Since the piezocatalytic reaction reactor is separated from the water medium by two glass barriers, the mechanical energy transmitted from the water into the reaction mixture is attenuated. The effective ultrasonic intensity **(I_S)** reaching the piezocatalyst-containing suspension is defined as:

$$I_S = (1 - 2R) \cdot P \cdot \left(\frac{V_S}{V_0}\right)$$

Here, P denotes the nominal ultrasonic power (160 W), and **V_S** is the volume of the reaction suspension (20 mL). The total mechanical energy input absorbed by the suspension during the reaction period (**t**, taken as 3600 seconds) is:

$$E_{mech} = I_S \cdot t$$

This model allows for a quantitative assessment of the mechanical energy effectively utilized in the piezocatalytic process by incorporating the geometric parameters of the ultrasonic system, the physical properties of materials involved, and the duration of treatment.

Table S1. Comparative literature overview of H_2 production performances and MTH efficiencies of reported piezocatalytic systems.

Catalyst	Conditions	H_2 production rate (μmol g^{-1} h^{-1})	MTH (%)	Ref.
LZO15	TEOA, 160 W, 35 kHz	1198	0.41%	This work
PTFE nanoparticles (CEC)	Pure water,	1286.6	0.17%	[1]
Bi_5O_7Br HNTs	Pure water	2456.48	0.28%	[2]
Bi_5O_7Br HNTs (seawater)	Seawater	1560.36	0.15%	[2]
$Bi_2O_2(OH)(NO_3)$ monolayer (BON-M)	Pure water, 240 W, 40 kHz	2071.05	0.19%	[3]
$Bi_2O_2(OH)(NO_3)$ monolayer (BON-M)	Seawater, 240 W, 40 kHz	1560.36	0.15%	[3]
$Bi_2O_2(OH)(NO_3)$ monolayer (BON-M)	Tap water, 240 W, 40 kHz	2237.62	0.21%	[3]
$Bi_2Fe_4O_9$ nanoplates	Pure water, 200 W, 40 kHz	1058	-	[4]
SnSe nanosheets	TEOA, 100 W, 45 kHz	948.4	-	[5]
Cd-doped $NiTiO_3$ nanotubes	Glucose, 200 W, 40 kHz	1520	-	[6]
Core/shell $CdS@SnS_2$ heterostructure	Na_2S and Na_2SO_3	452.6	-	[7]
CdS/BiOCl S-scheme heterojunction	Methanol, 120 W	1048.2	-	[8]
CdS/Bi_2WO_6	Methanol, 150 W, 40 kHz	1020	-	[9]

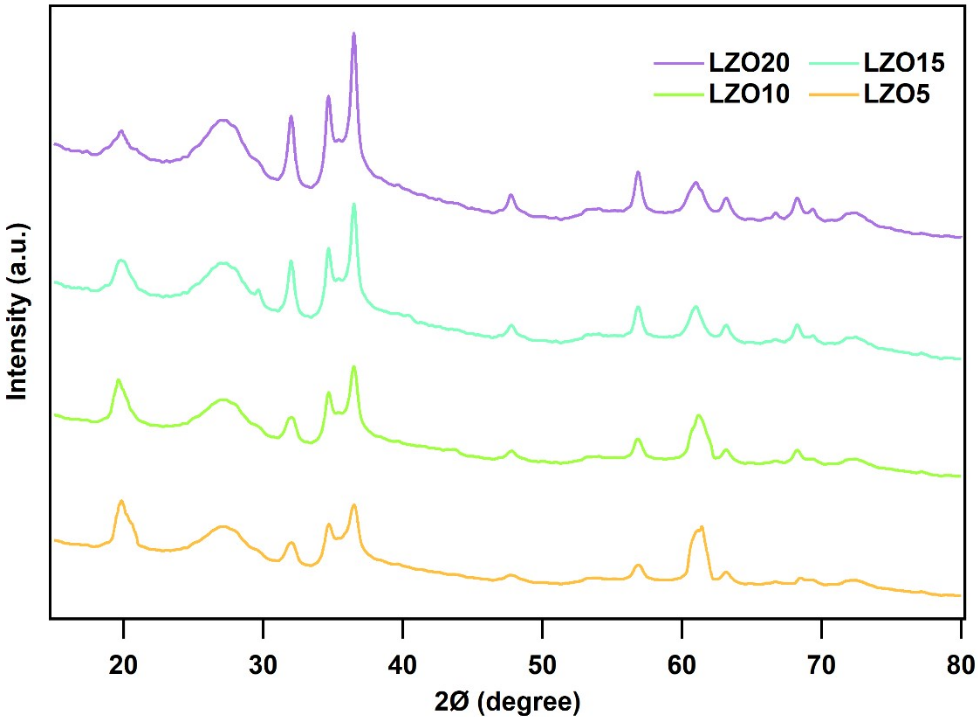

Figure S1. XRD patterns of LZO5, LZO10, LZO15 and LZO20 composites.

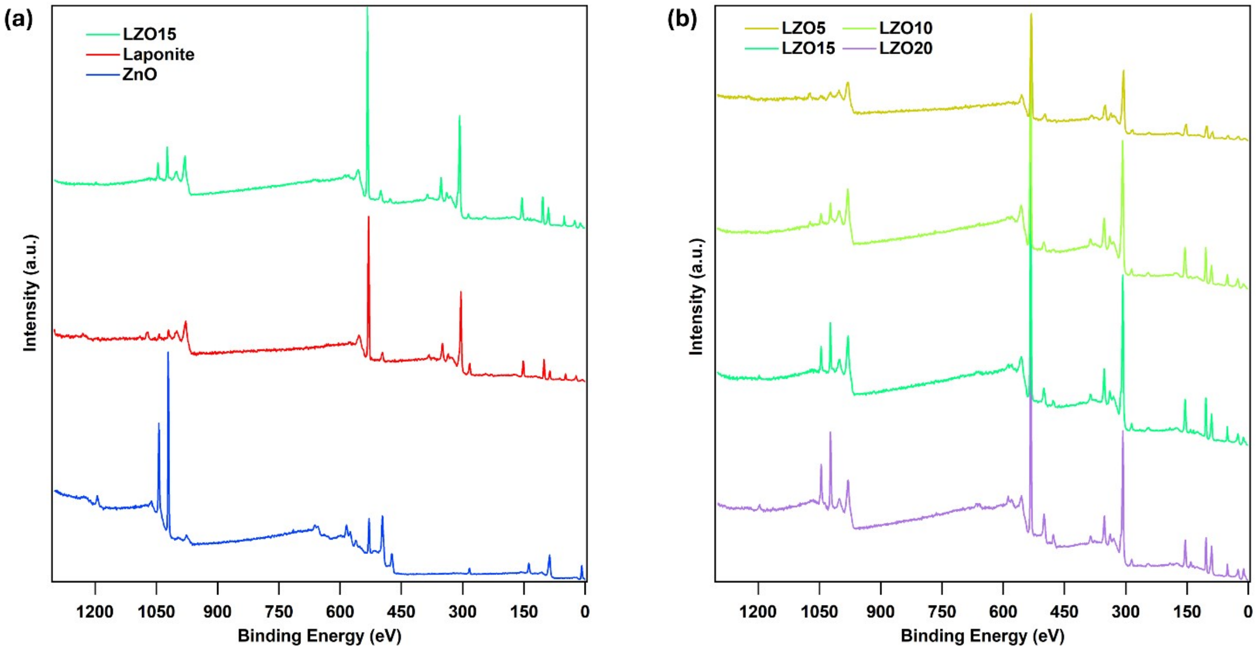

Figure S2. (a) XPS survey spectra of Laponite, ZnO and LZO15. (b) XPS survey spectra of LZO5, LZO10, LZO15, and LZO20.

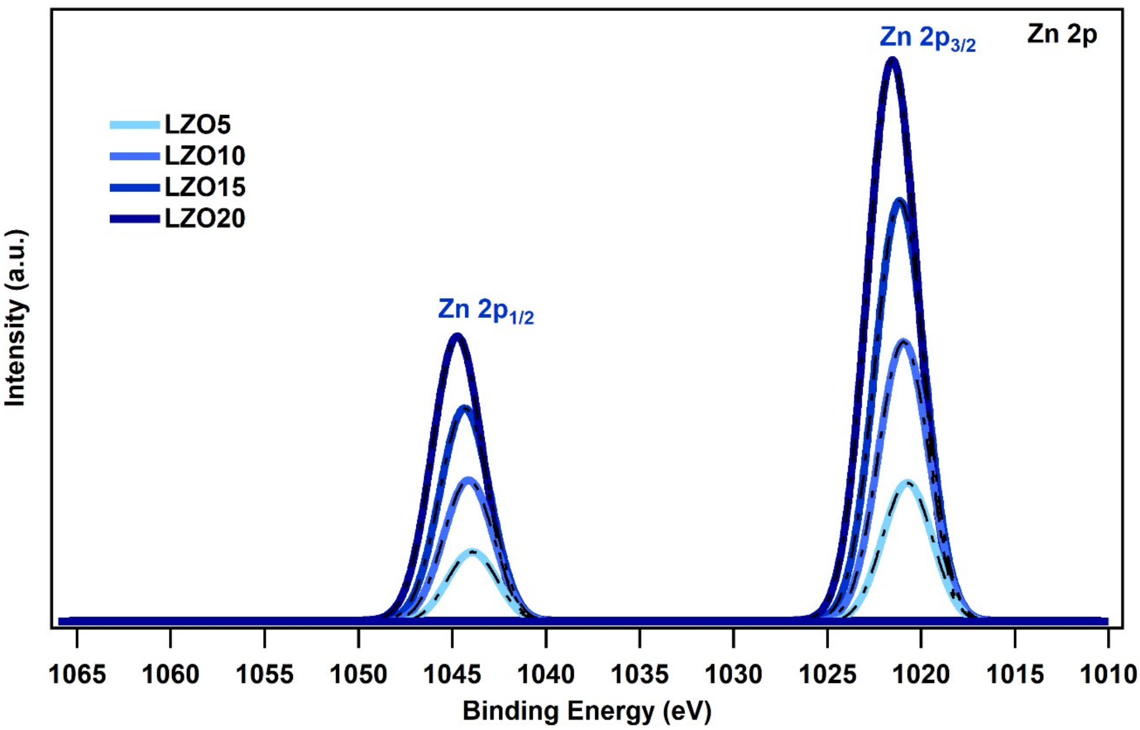

Figure S3. High resolution XPS spectra of Zn 2p belonging to LZO5, LZO10, LZO15 and LZO20 composites.

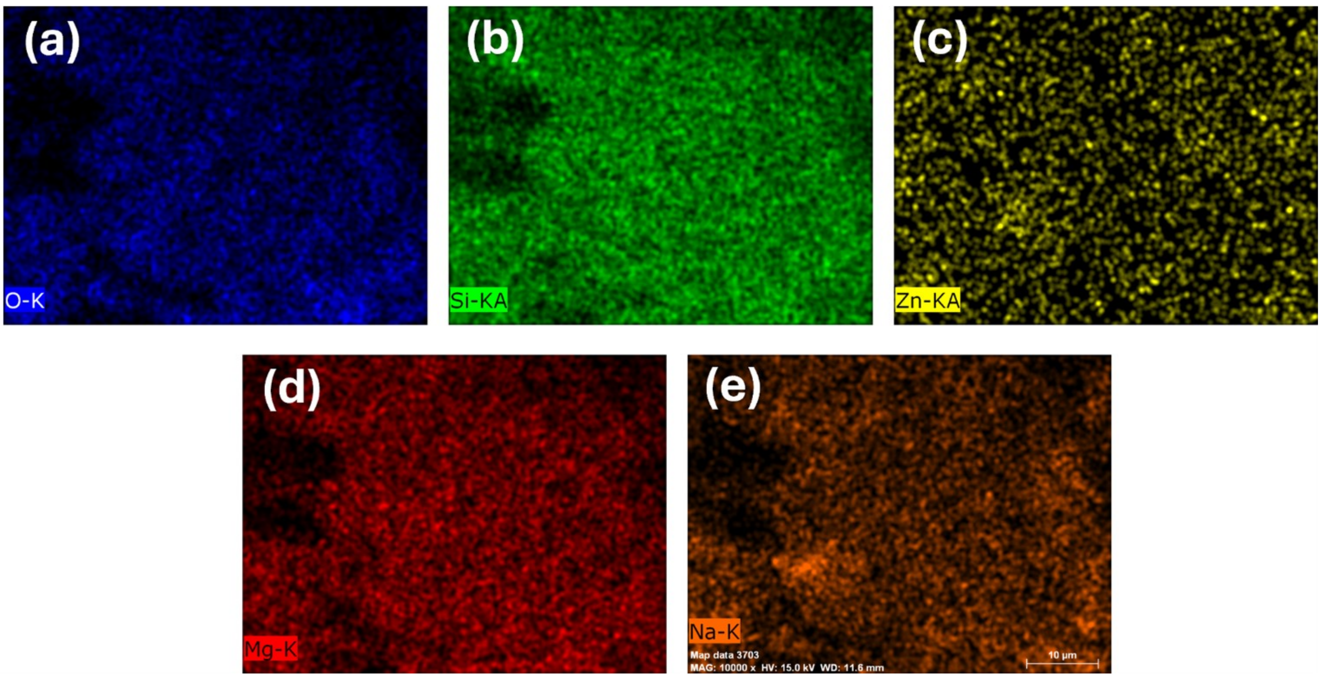

Figure S4. Elemental mapping images of LZO15 for (a) O, (b) Si, (c) Zn, (d) Mg, and (e) Na

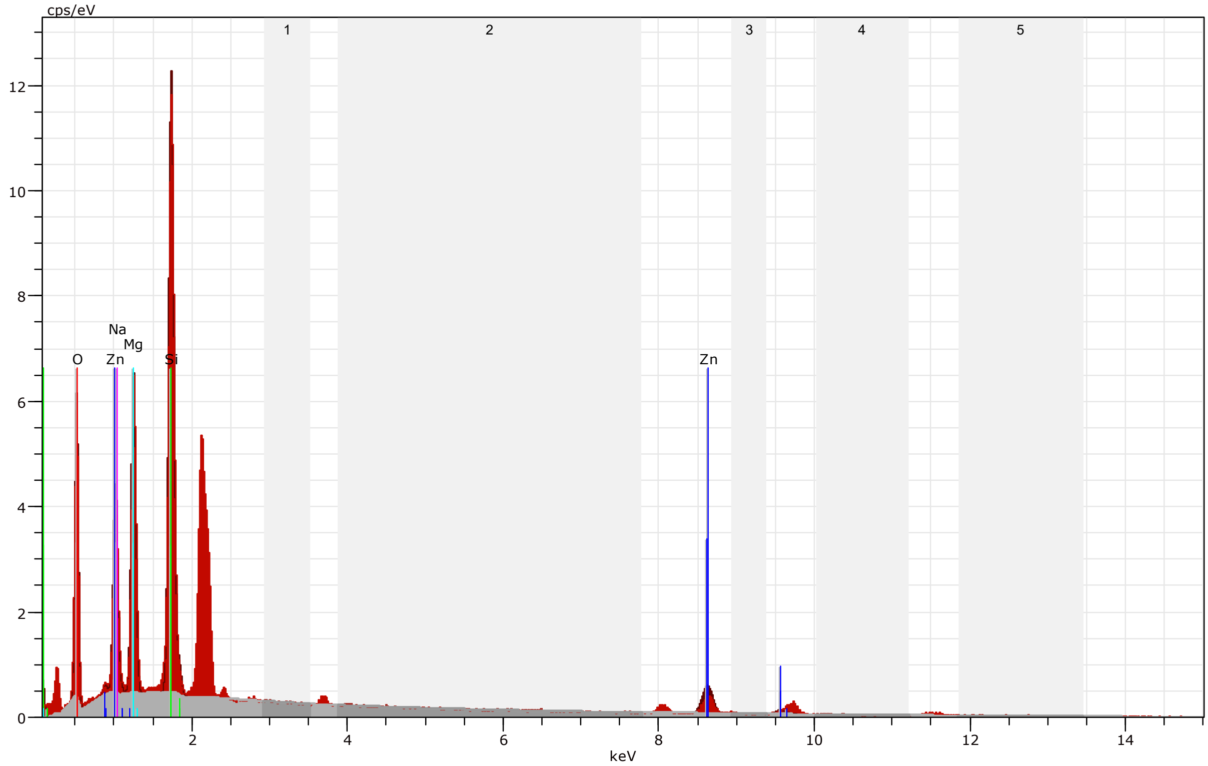

Figure S5. Energy Dispersive X-ray Spectroscopy (EDX) result of LZO15.

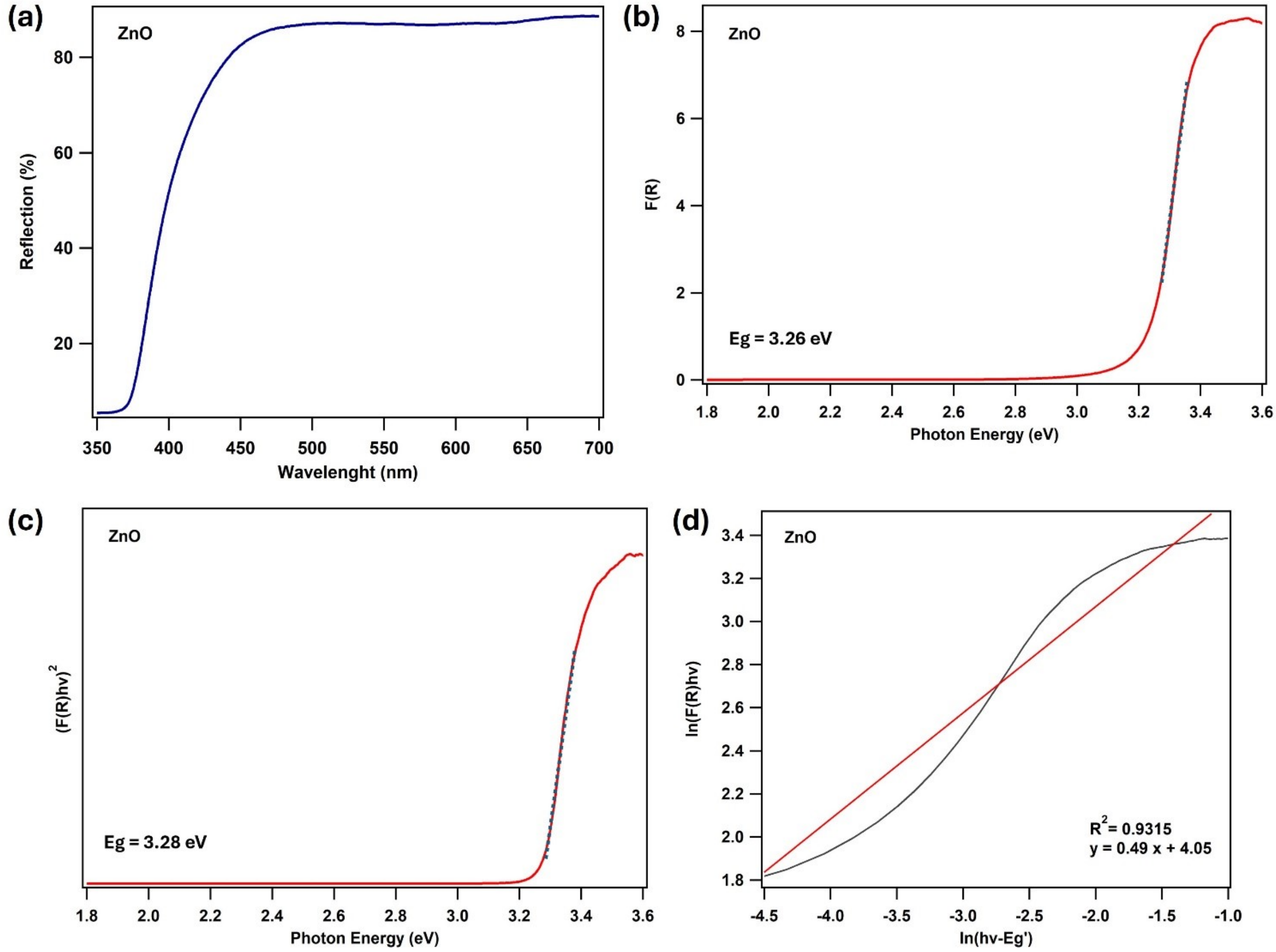

Figure S6. Diffuse reflectance plot (a), F(R) vs photon energy (b), ln(F(R)hυ) - ln(hυ-Eg’) graphs (c) and band gap energy diagram (d) of ZnO.

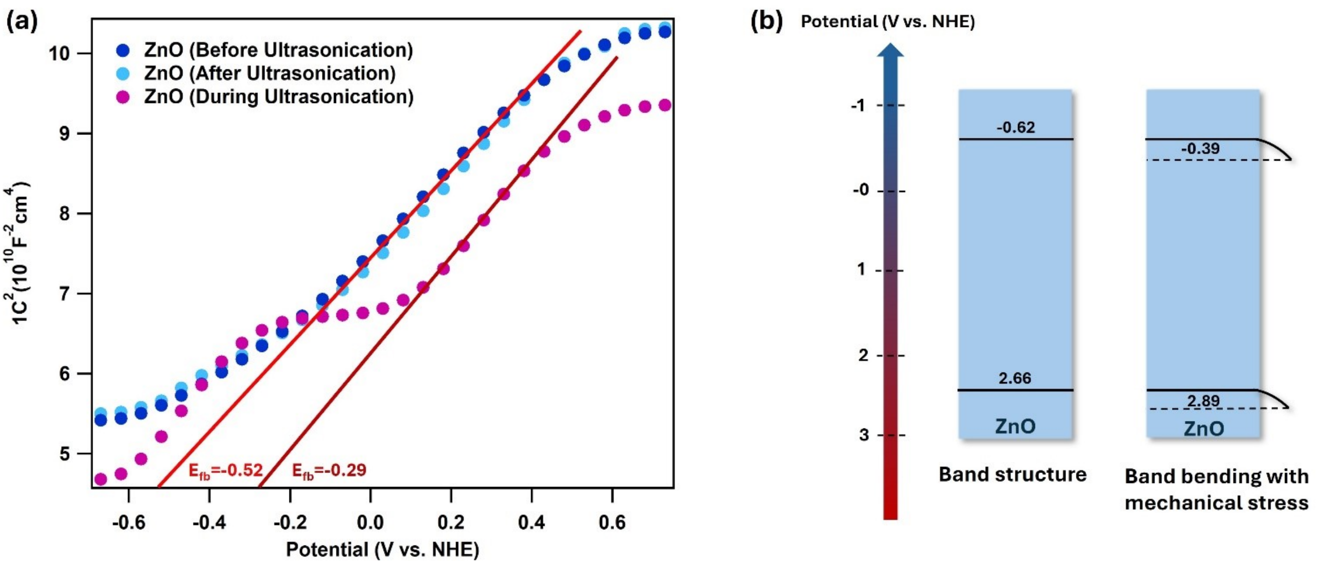

Figure S7. Mott-Schottky plot of (a) ZnO measured by using 0.1 M $NaSO_4$ supporting electrolyte in the absence and presence of ultrasonication. (b) Band-gap diagram and band bending under mechanical stress

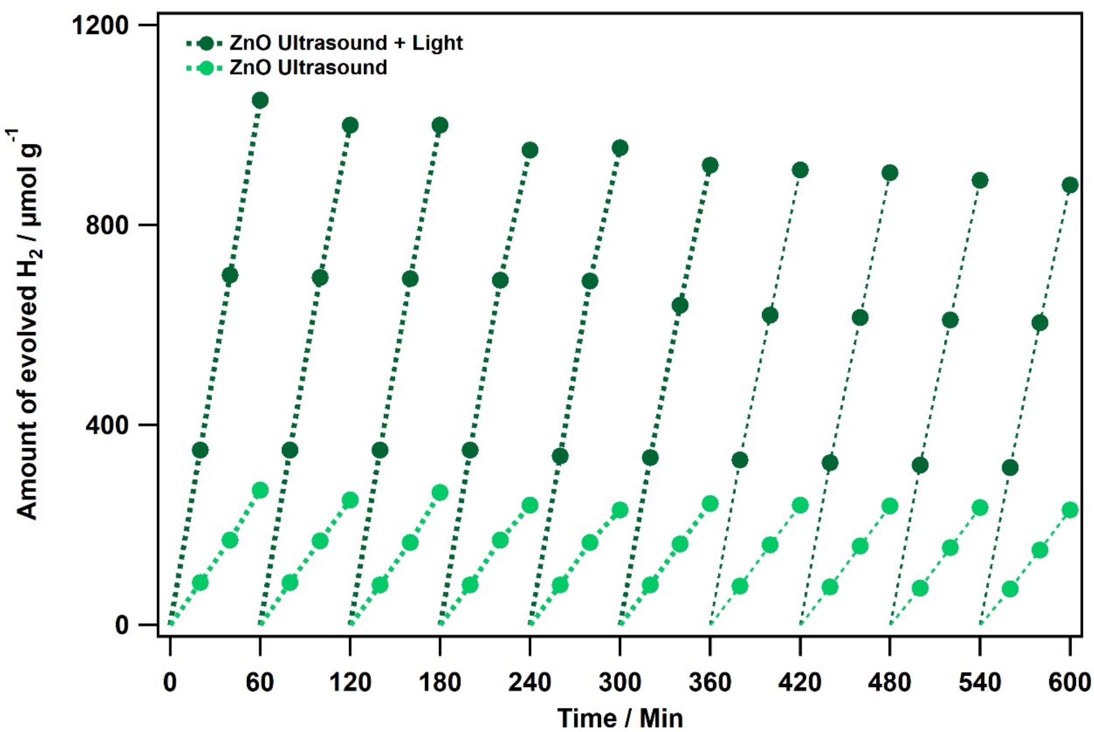

Figure S8. Reusability experiments for photo/piezocatalytic hydrogen production of ZnO for 10 cycles.

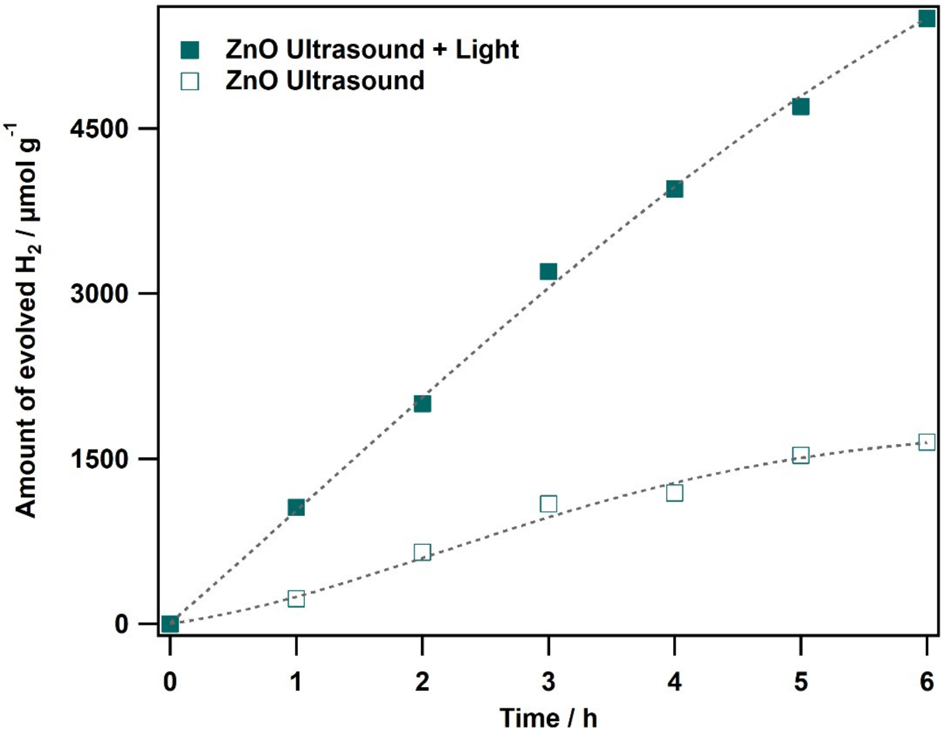

Figure S9. Long-Term photo/piezocatalytic hydrogen production of ZnO for 6 hours.

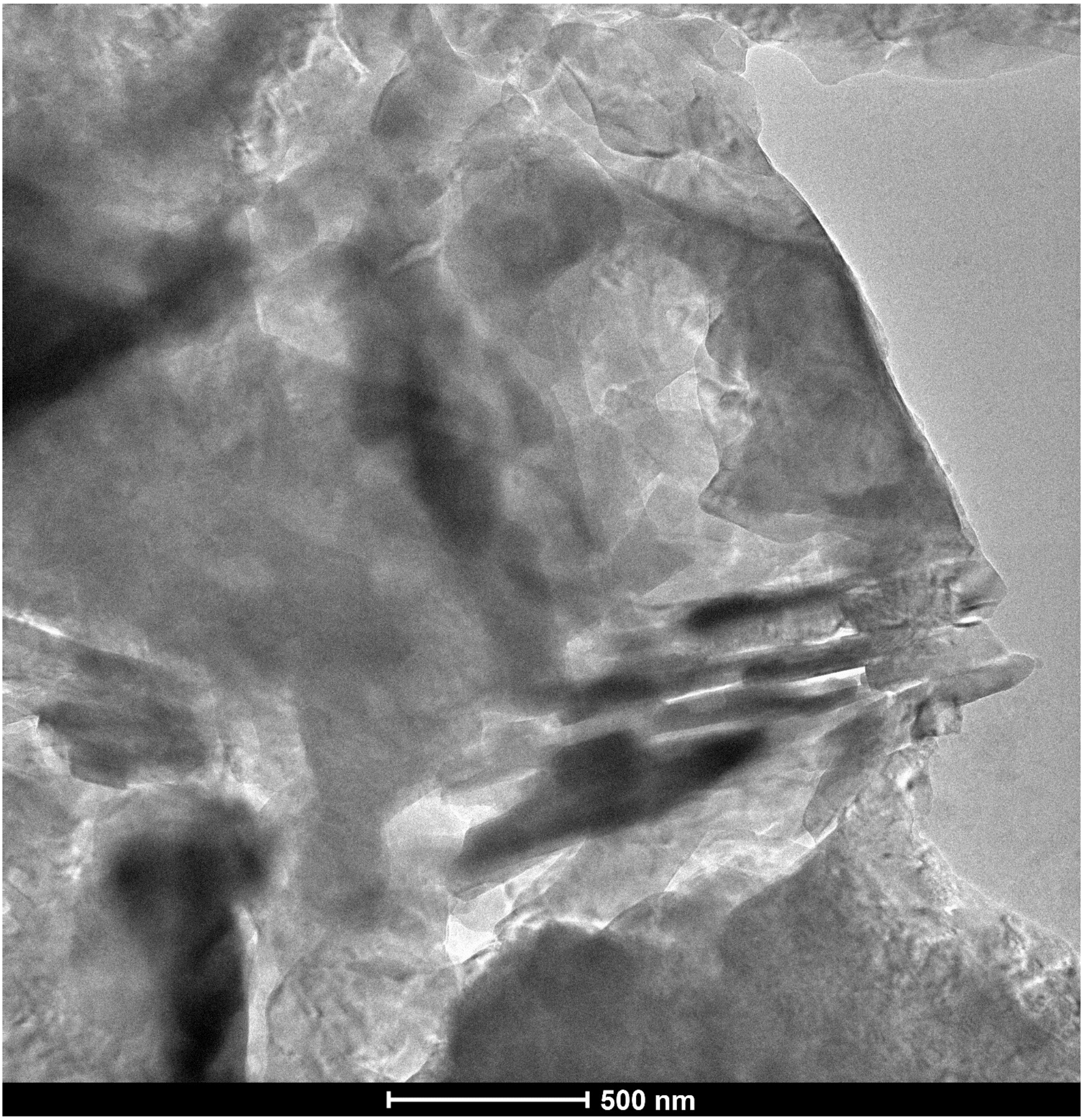

Figure S10. TEM image of LZO15 catalyst recovered from the reaction medium after 10 cycles test

REFERENCES

1. N. Tian, J. Kuang, C. Yuan, X. Zhang, Y. Zhang and H. Huang, *Journal of Materials Chemistry A*, 2025, **13**, 32344-32350.
2. C. Wang, F. Chen, E. Chen, T. Chen, T. Ma and H. Huang, *ACS nano*, 2025.
3. C. Wang, S. Tu, F. Chen, T. Ma and H. Huang, *Advanced Materials*, 2025, 2505592.
4. Y. Du, T. Lu, X. Li, Y. Liu, W. Sun, S. Zhang and Z. Cheng, *Nano Energy*, 2022, **104**, 107919.
5. S. Li, Z. Zhao, J. Li, H. Liu, M. Liu, Y. Zhang, L. Su, A. I. Pérez-Jiménez, Y. Guo, F. Yang, Y. Liu, J. Zhao, J. Zhang, L.-D. Zhao and Y. Lin, *Small*, 2022, **18**, 2202507.
6. K. Li, B. Li, X. Zhang, J. Wu, M. Chen, P. Feng, X. Yang, M. Zhang and Y. Ding, *Chem. Commun.*, 2024, **60**, 4801-4804.
7. R. Xiong, Y. Song, K. Li, Y. Xiao, B. Cheng and S. Lei, *J. Mater. Chem. A*, 2023, **11**, 18398-18408.
8. P. Hao, Y. Cao, X. Ning, R. Chen, J. Xie, J. Hu, Z. Lu and A. Hao, *J. Colloid Interface Sci.*, 2023, **639**, 343-354.
9. X. Ning, A. Hao and X. Qiu, *Advanced Functional Materials*, 2025, **35**, 2413217.